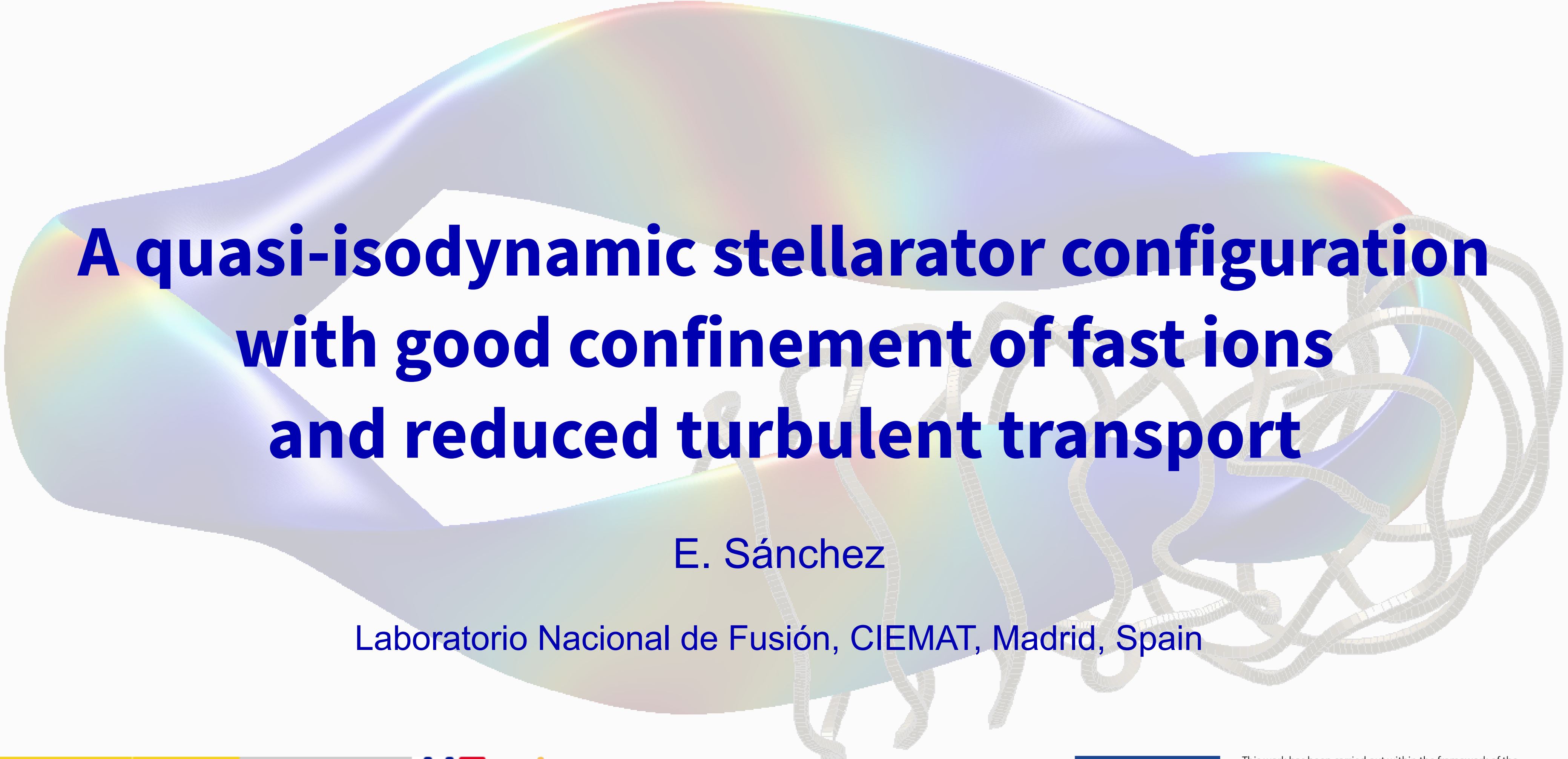

A quasi-isodynamic stellarator configuration with good confinement of fast ions and reduced turbulent transport

E. Sánchez

Laboratorio Nacional de Fusión, CIEMAT, Madrid, Spain

GOBIERNO DE ESPAÑA
MINISTERIO DE CIENCIA E INNOVACIÓN
Ciemat
Centro de Investigaciones Energéticas, Medioambientales y Tecnológicas
UE 23
Laboratorio Nacional de Fusión
Ciemat
EUROfusion

This work has been carried out within the framework of the EUROfusion Consortium, funded by the European Union via the Euratom Research and Training Programme (Grant Agreement No 101052200 — EUROfusion). Views and opinions expressed are however those of the author(s) only and do not necessarily reflect those of the European Union or the European Commission. Neither the European Union nor the European Commission can be held responsible for them.

European Fusion Theory Conference, October 2-4, Padova, Italy

Collaborators

J.L. Velasco, I. Calvo, J. M. García-Regaña, A. Alonso, I. Palermo, I. Fernández,

D. Carralero, M. Medrano, J. Alonso, S. Cabrera, P. Méndez, E. Rincón, Á. Cappa,
J. Martínez, D. Rapisarda, F. R. Urgorri, Á. Ibarra, F. Tabarés, G. Godino, S. Mulas.
Laboratorio Nacional de Fusión, CIEMAT.

Thanks to

M. Landreman, E. Paul, H. Yamaguchi, C. Zhu, S. Lazerson, C. Beidler, M. Drevlak, Y. Suzuki.

Outline of the talk

- Motivation an theory
- Goals
- Results
- Summary

Motivation

- The stellarator concept offers advantages with respect to the tokamak.
  - Most of the current is externally generated (no current instabilities or disruptions).
  - Easier steady state operation.
- Magnetic field in a stellarator is intrinsically three-dimensional.
  - More complex phenomenology than in tokamaks.
  - Good confinement requires careful tailoring of the magnetic field (optimization).

Motivation

- The stellarator concept offers advantages with respect to the tokamak.
  - Most of the current is externally generated (no current instabilities or disruptions).
  - Easier steady state operation.
- Magnetic field in a stellarator is intrinsically three-dimensional.
  - More complex phenomenology than in tokamaks.
  - Good confinement requires careful tailoring of the magnetic field (optimization).

W7-X: the largest optimized stellarator.

✢ Good confinement of thermal ions demonstrated in W7-X [Beidler, Nature 2021].

Great success ! But

- Turbulence limits performance in most plasma scenarios [Bozhenkov NF20, Beurskens NF21, Carralero NF21].
- Fast ion confinement is not good enough for a reactor, some improvement expected with with β (to be confirmed) [Drevlak, NF 2014].

→ **These two aspects require improvement (optimization) for a stellarator reactor design.**

W7-X at Max Planck IPP Greifswald

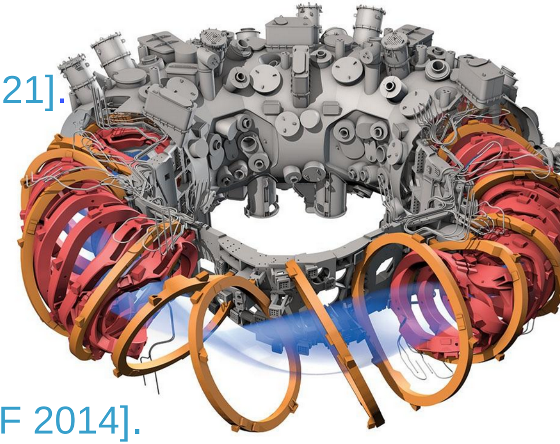

Optimization via omnigenous fields

- Charged particles in an inhomogeneous magnetic field drift perpendicularly to the magnetic field.
- A magnetic field is called **omnigenous** if the orbit-averaged radial magnetic drift vanishes ($\overline{\mathbf{v}_M \cdot \nabla r} = 0$) for all particles [Cary PoP 1997].

  If this property is fulfilled, collisionless particles are confined.
  - Thanks to axisymmetry, this is ensured in a tokamak.
  - It is not automatically fulfilled in a general stellarator and requires optimization.

- Trapped particles move keeping constant its energy, magnetic moment and second adiabatic invariant (J).

$$J = \int_{l_{b_1}}^{l_{b_2}} |v_{\|}| dl$$

- The orbit average of the magnetic drift can be expressed in terms of derivatives of J.

$$\overline{\mathbf{v}_M \cdot \nabla r} \sim \partial_\alpha J \qquad \overline{\mathbf{v}_M \cdot \nabla \alpha} \sim -\partial_r J$$

=> J **is constant on flux surface in a omnigenous field**.

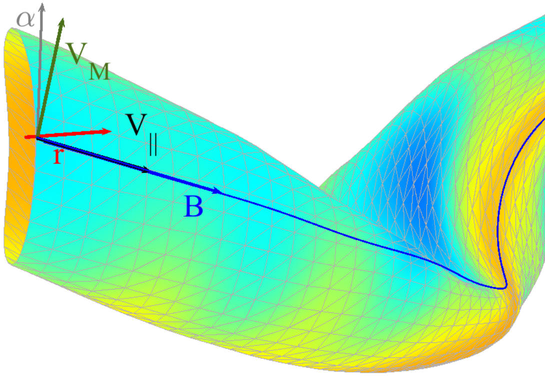

v_M := magnetic drift
$V_{\|}$:= parallel (to B) component of velocity
α := field line label
r := radial coordinate
l:= coordinate along the field line
l_{b1}, l_{b2} := bounce points of a trapped-particle trajectory

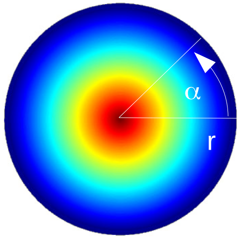

Contours of ***second adiabatic invariant*** *J for an omnigenous* ***configuration in polar coordinates (r, α)****.*

Types of omnigeneity

- **Quasi-symmetric (QS)** devices. The magnetic field strength has a symmetry along the toroidal (QA) or a helical direction (QH).
  - **HSX** (QH) [Anderson FT 1995],
  - **NCSX** (QA) [Zarnstorff PPCF 2001],
  - **CFQS** (QA) [Liu NF 2021].
  - More recent QS configurations [Ku FST 2006, Ku NF 2011, Henneberg NF 2019, Bader JPP 2020, Jorge NF 2020, Landreman PRL 2022, Landreman PoP 2022] …
- **Quasi-isodynamic (QI)** devices. No explicit symmetry; |**B**| contours close poloidally.
  - **W7-X** [Grieger FT 1992] is the most prominent example of this concept.
  - More recent QI configurations [Mikhailov NF 2002, Subbotin NF 2006, Mikhailov PPR 2009, Plunk JPP 2019, Jorge JPP 2022, Camacho JPP 2022, Jorge PPCF 2023, Goodman JPP 2023, Dudt arXiv 2023]…

Advantage of QI over the QS concept: **the bootstrap current is small** [Helander PPCF 2009], which allows better control of the rotational transform profile (island divertor).

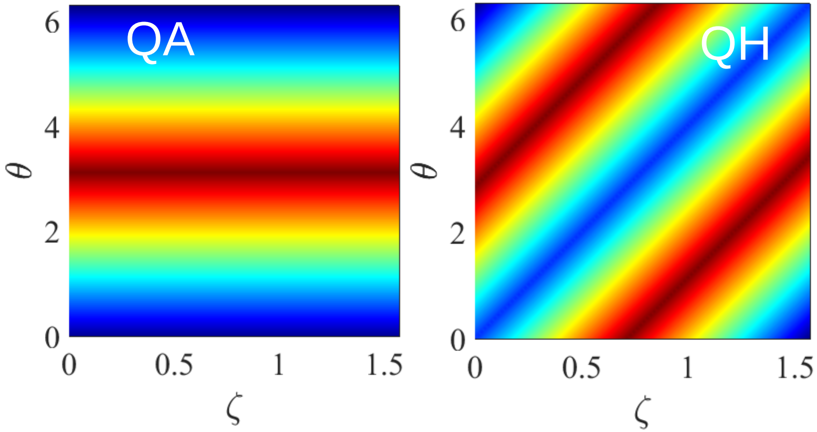

Magnetic field strength over a flux surface versus Boozer angle coordinates for a QA (top left), QH (top right) and a QI (bottom) configuration

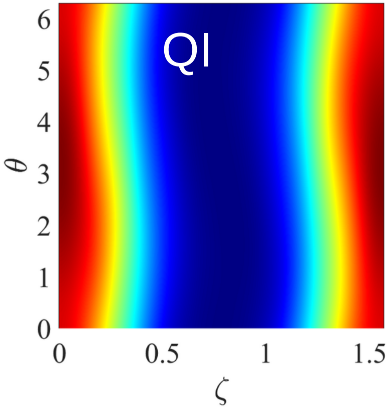

Types of omnigeneity

- **Quasi-symmetric (QS)** devices. The magnetic field strength has a symmetry along the toroidal (QA) or a helical direction (QH).
  - **HSX** (QH) [Anderson FT 1995],
  - **NCSX** (QA) [Zarnstorff PPCF 2001],
  - **CFQS** (QA) [Liu NF 2021].
  - More recent QS configurations [Ku FST 2006, Ku NF 2011, Henneberg NF 2019, Bader JPP 2020, Jorge NF 2020, Landreman PRL 2022, Landreman PoP 2022]…

- **Quasi-isodynamic (QI)** devices. No explicit symmetry; **|B|** contours close poloidally.
  - **W7-X** [Grieger FT 1992] is the most prominent example of this concept.
  - More recent QI configurations [Mikhailov NF 2002, Subbotin NF 2006, Mikhailov PPR 2009, Plunk JPP 2019, Jorge JPP 2022, Camacho JPP 2022, Jorge PPCF 2023, Goodman JPP 2023, Dudt arXiv 2023]...

Advantage of QI over the QS concept: **the bootstrap current is small** [Helander PPCF 2009], which allows better control of the rotational transform profile (island divertor).

The traditional approach has been reducing $\overline{\mathbf{v}_M \cdot \nabla r}$ as much as possible, through a careful design of $B(\theta, \zeta)$, but this is not enough.

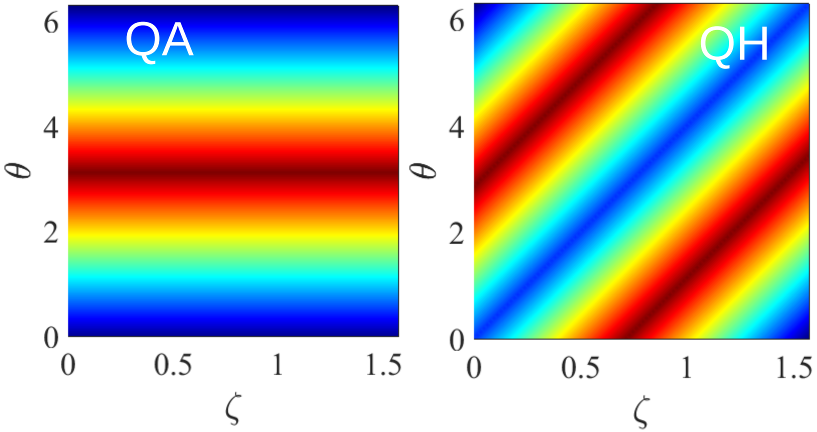

Magnetic field strength over a flux surface versus Boozer angle coordinates for a QA (top left), QH (top right) and a QI (bottom) configuration

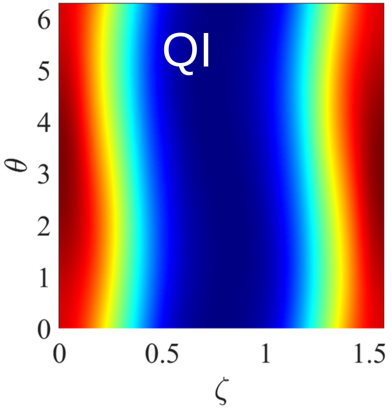

Outline of the talk

- Motivation an theory
- Goals
- Results
- Summary

Robust optimization via flat mirror term

- Reducing $|\overline{\mathbf{v}_M \cdot \nabla r}|$ is not enough.
  - Finite β effect and error fields from the coils can increase it.
  - Having finite (large) $|\overline{\mathbf{v}_M \cdot \nabla \alpha}|$ improves the confinement of collisionless particles.

Robust optimization via flat mirror term

- Reducing $|\overline{\mathbf{v}_M \cdot \nabla r}|$ is not enough.
  - Finite β effect and error fields from the coils can increase it.
  - Having finite (large) $|\overline{\mathbf{v}_M \cdot \nabla \alpha}|$ improves the confinement of collisionless particles.
- Finite $\overline{\mathbf{v}_M \cdot \nabla \alpha} \sim -\partial_r J$ can be obtained through a small radial variation of the mirror term (**flat mirror**) [Velasco arXiv:2306.17506v1].

$$B_M(s) := \sum_{n>0} B_{0n}(s)$$

Several positive consequences:

  - Increases $|\overline{\mathbf{v}_M \cdot \nabla \alpha}|$ and voids $\partial_r J = 0$ => Reduced fast ion losses.
  - Allows achieving maximum-*J* ($\partial_r J < 0$) => Reduced turbulent TEM transport [Rosenbluth PoF 1968, Helander PoP 2013].
  - Positive impact on neoclassical confinement [Velasco arXiv:2306.17506v1].
  - Positive impact on impurity acumulation [Velasco arXiv:2306.17506v1].
  - These properties **can be achieved without being very close to QI (robust optimization), in particular at low (and high) β.**
    - Traditionally, having maximum-*J* property relied on having high β.

Sketch of a magnetic field with the flat mirrror property

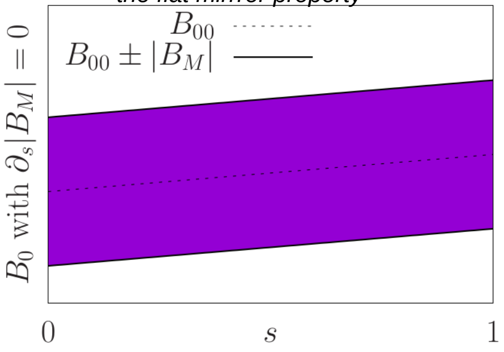

Sketch of a magnetic field without the flat mirrror property

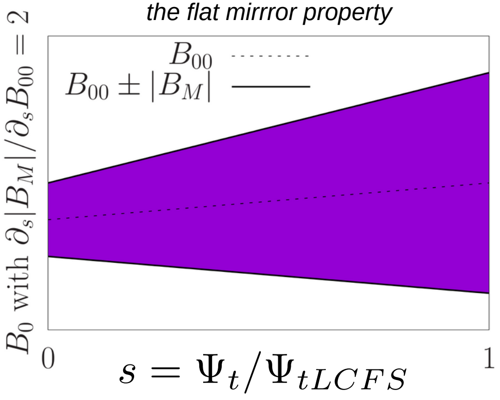

See Velasco P2.11 This conference.

Our optimization goal

- We seek a **maximum-*J* QI configuration at low and high β.**
  - **QI**: omnigenous magnetic field ($\overline{\mathbf{v}_M \cdot \nabla r} = 0$) + poloidally closed B contours.
    - low neoclassical transport.
    - good confinement of fast ions.
    - reduced bootstrap current.

$$\overline{\mathbf{v}_M \cdot \nabla r} \sim \partial_\alpha J$$

Magnetic field strength versus Boozer coordinates for a QI configuration

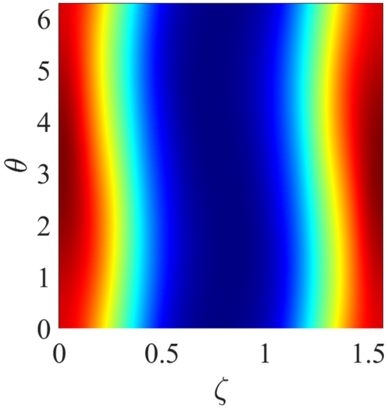

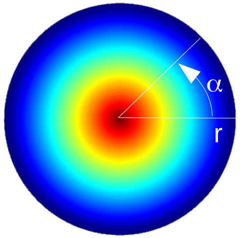

*Contours of **second adiabatic invariant** J for E/μ=B_{00} for a **QI configuration**.*

Our optimization goal

- We seek a **maximum-*J* QI configuration at low and high β.**
  - **QI**: omnigenous magnetic field ($\overline{\mathbf{v}_M \cdot \nabla r} = 0$) + poloidally closed B contours.
    - low neoclassical transport.
    - good confinement of fast ions.
    - reduced bootstrap current.
  - **Maximum-*J*** property: $\overline{\mathbf{v}_M \cdot \nabla \alpha} > 0$ for all particles.
    - reduced TEM turbulence.
    - beneficial for other ion-scale instabilities.

$$\overline{\mathbf{v}_M \cdot \nabla r} \sim \partial_\alpha J$$

$$\overline{\mathbf{v}_M \cdot \nabla \alpha} \sim -\partial_r J$$

Magnetic field strength versus Boozer coordinates for a QI configuration

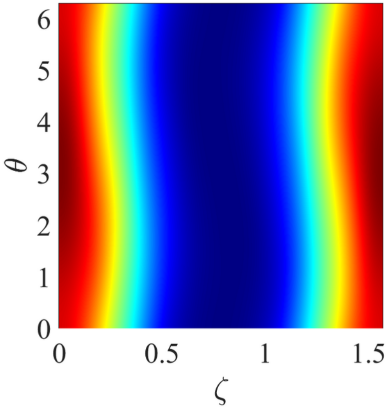

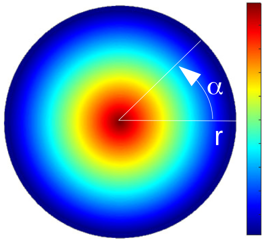

*Contours of **second adiabatic invariant** J for E/μ=B_{00} for a **QI configuration with maximum-J**.*

Our optimization goal

- We seek a **maximum-*J* QI configuration at low and high β.**
  - **QI**: omnigenous magnetic field ($\overline{\mathbf{v}_M\cdot\nabla r}=0$) + poloidally closed B contours.
    - low neoclassical transport.
    - good confinement of fast ions.
    - reduced bootstrap current.
  - **Maximum-*J*** property: $\overline{\mathbf{v}_M\cdot\nabla\alpha}>0$ for all particles.
    - reduced TEM turbulence.
    - beneficial for other ion-scale instabilities.
    - good confinement of fast ions even if not very close to exact QI.
    - NEW: good confinement of bulk ions even if not very close to exact QI.

$$\left|\frac{\overline{\mathbf{v}_M\cdot\nabla r}}{\overline{\mathbf{v}_M\cdot\nabla\alpha}}\right|=\left|\frac{\partial_\alpha J}{\partial_r J}\right|<<1$$

Magnetic field strength versus Boozer coordinates for a QI configuration

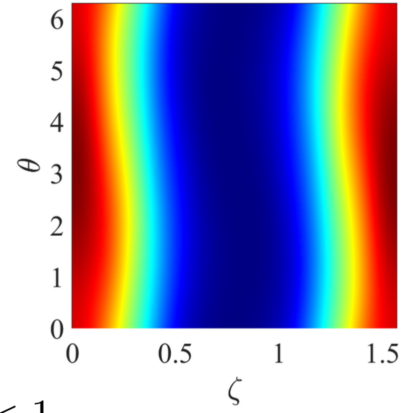

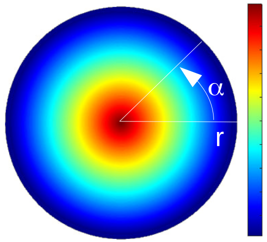

Contours of ***second adiabatic invariant*** *J for $E/\mu=B_{00}$ for a* ***QI configuration with maximum-J****.*

Our optimization goal

- We seek a **maximum-*J* QI configuration at low and high β.**
  - **QI**: omnigenous magnetic field ($\overline{\mathbf{v}_M \cdot \nabla r} = 0$) + poloidally closed B contours.
    - low neoclassical transport.
    - good confinement of fast ions.
    - reduced bootstrap current.
  - **Maximum-*J*** property: $\overline{\mathbf{v}_M \cdot \nabla \alpha} > 0$ for all particles.
    - reduced TEM turbulence.
    - beneficial for other ion-scale instabilities.
    - good confinement of fast ions even if not very close to exact QI.
    - NEW: good confinement of bulk ions even if not very close to exact QI.

$$\left|\frac{\overline{\mathbf{v}_M \cdot \nabla r}}{\overline{\mathbf{v}_M \cdot \nabla \alpha}}\right| = \left|\frac{\partial_\alpha J}{\partial_r J}\right| << 1$$

  - **We know we can approach maximum-*J* already at low β** [Velasco arXiv:2306.17506v1].
  - **Reduced turbulence and good confinement of fast ions at low β** can be important for a reactor.
    - Reduced auxiliary heating required to reach operation point [Alonso NF 2022].
    - Reduced wall load during power ramp up.

Magnetic field strength versus Boozer coordinates for a QI configuration

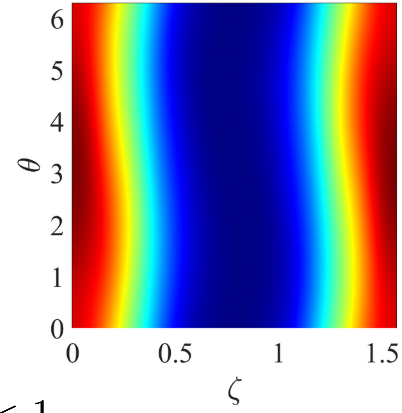

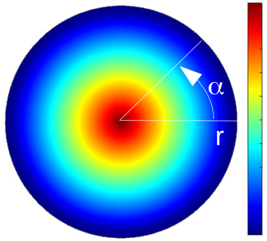

*Contours of **second adiabatic invariant** J for $E/\mu=B_{00}$ for a **QI configuration with maximum-J**.*

Our optimization goal

Laboratorio Nacional de Fusión
Ciemat

- We seek a **maximum-*J* QI configuration at low and high β.**
  - **QI**: omnigenous magnetic field ($\overline{\mathbf{v}_M \cdot \nabla r} = 0$) + poloidally closed B contours.
    - low neoclassical transport.
    - good confinement of fast ions,
    - reduced bootstrap current.
  - **Maximum-*J*** property: $\overline{\mathbf{v}_M \cdot \nabla \alpha} > 0$ for all particles.
    - reduced TEM turbulence.
    - beneficial for other ion-scale instabilities.
    - good confinement of fast ions even if not very close to exact QI.
    - NEW: good confinement of bulk ions even if not very close to exact QI.

$$\left|\frac{\overline{\mathbf{v}_M \cdot \nabla r}}{\overline{\mathbf{v}_M \cdot \nabla \alpha}}\right| = \left|\frac{\partial_\alpha J}{\partial_r J}\right| << 1$$

  - ✛ **We know we can approach maximum-*J* already at low β** [Velasco arXiv:2306.17506v1].
  - ✛ **Reduced turbulence and good confinement of fast ions at low β** can be important for a reactor.
    - Reduced auxiliary heating required to reach operation point [Alonso NF 2022].
    - Reduced wall load during power ramp up.
- Aditionally, we require:
  - MHD stability,
  - ι profile compatible with island divertor and avoiding low order rationals,
  - Coils.

Magnetic field strength versus Boozer coordinates for a QI configuration

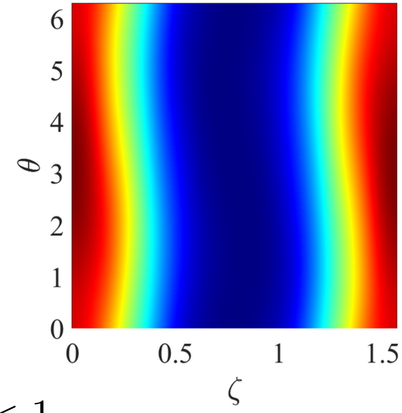

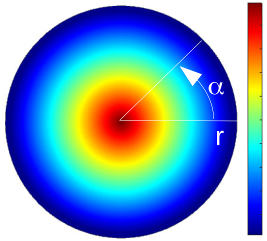

*Contours of **second adiabatic invariant** J for E/μ=B$_{00}$ for a **QI configuration with maximum-J**.*

Tools and strategy

- STELLOP suite of codes is our workhorse.
    - KNOSOS [Velasco et al. JCP 2020] has been integrated into STELLOPT and is used for evaluating orbit-averaged quantities used as metrics of QI and maximum-*J* (https://github.com/PrincetonUniversity/STELLOPT/tree/CIEMAT).

Main targets used to approach the goals:

- Rotational transform.
- Magnetic well → ideal MHD stability.
- Effective ripple ε_{eff} → Ominigeneity.
- Alignment of B maxima and minima along poloidal contours → QI.
- Γ_c [Nemov et al. PoP 2008] + Γ_α [Velasco et al. NF 2021] → maximum-*J*.

The optimization of bootstrap current and turbulence relies on QI and maximum-*J* respectively.

Outline of the talk

- Motivation an theory
- Goals
- Results
- Summary

Optimized configuration: CIEMAT-QI

The first **quasi-isodynamic configuration** having (**simultaneously**):

Sánchez et al. 2023 Nucl. Fusion 63 066037

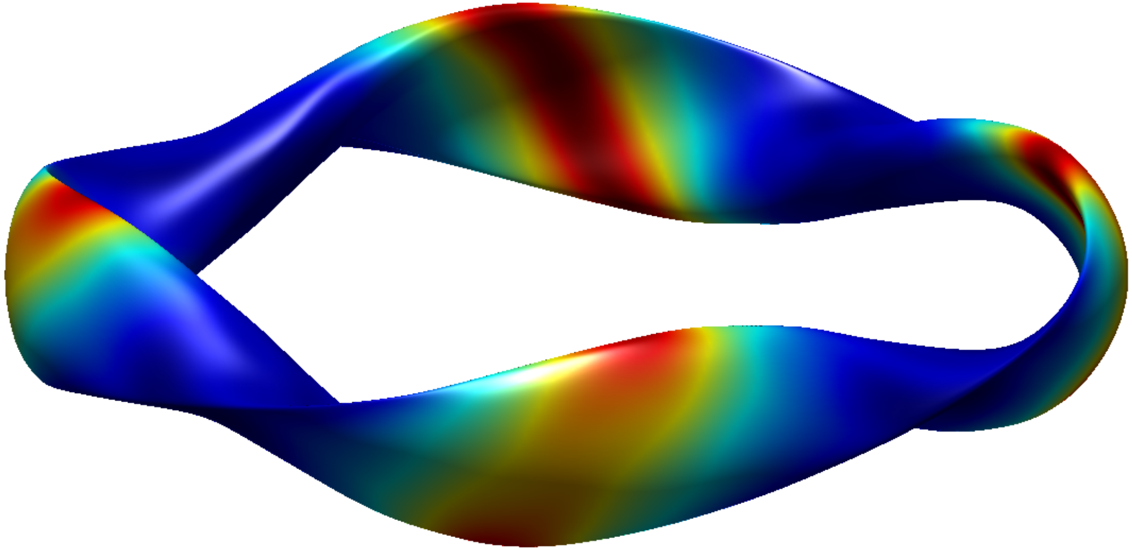

Magnetic field strength over the last closed flux surface for the optimized configuration with A=9.9, β=1.5%

- ι profile avoiding low order rationals and compatible with island divertor,

- Ideal MHD stability,

- Low neoclassical transport,

- Reduced bootstrap current,

+ Very good confinement of fast ions at low β (~1.5%),

+ Excellent confinement of fast ions at reactor-scale β (~4%),

+ Reduced turbulent transport.

+ Set of filamentary coils.

QI flat mirror configuration (see Velasco, Calvo, Sánchez et al. *Robust stellarator optimization via flat mirror magnetic fields*. arXiv:2306.17506v1).

Optimized configuration: CIEMAT-QI4

The first **quasi-isodynamic configuration** having (**simultaneously**):

Sánchez et al. 2023 Nucl. Fusion 63 066037

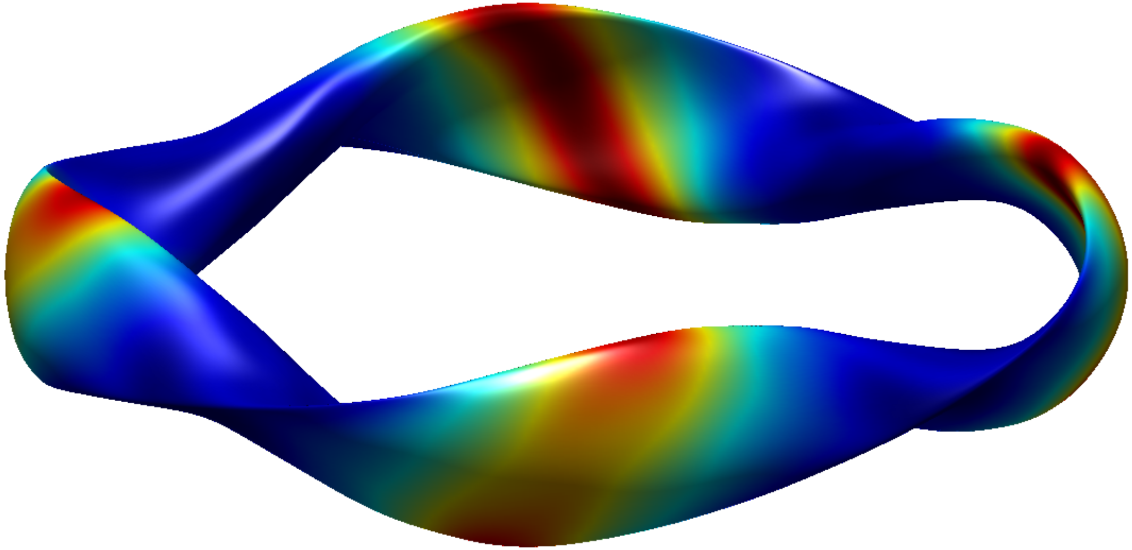

Magnetic field strength over the last closed flux surface for the optimized configuration with A=9.9, β=1.5%

- ι profile avoiding low order rationals and compatible with island divertor,

- Ideal MHD stability,

- Low neoclassical transport,

- Reduced bootstrap current,

+ Very good confinement of fast ions at low β (~1.5%),

+ Excellent confinement of fast ions at reactor-scale β (~4%),

+ Reduced turbulent transport.

+ Set of filamentary coils.

QI flat mirror configuration (see Velasco, Calvo, Sánchez et al. *Robust stellarator optimization via flat mirror magnetic fields*. arXiv:2306.17506v1).

Velasco, P2.11 and Godino-Sedano, P2.24. This conference.

Rotational transform and magnetic well

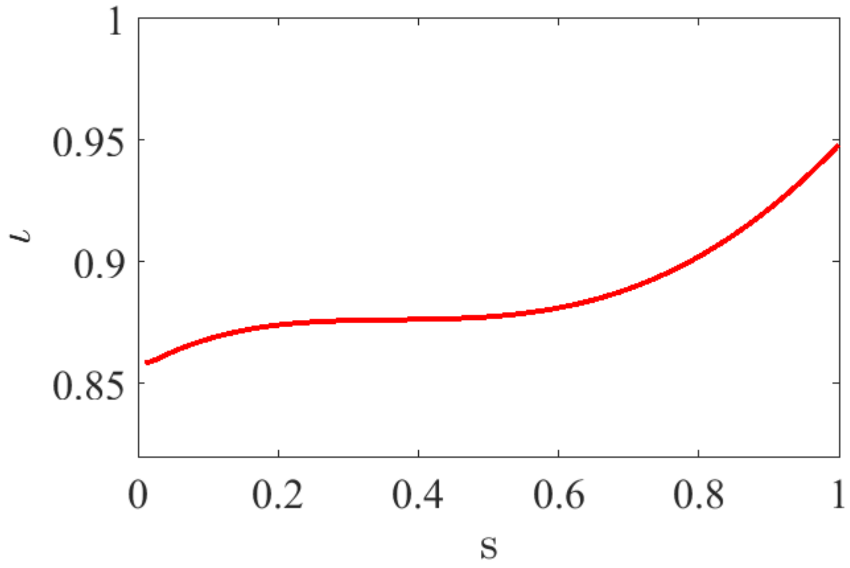

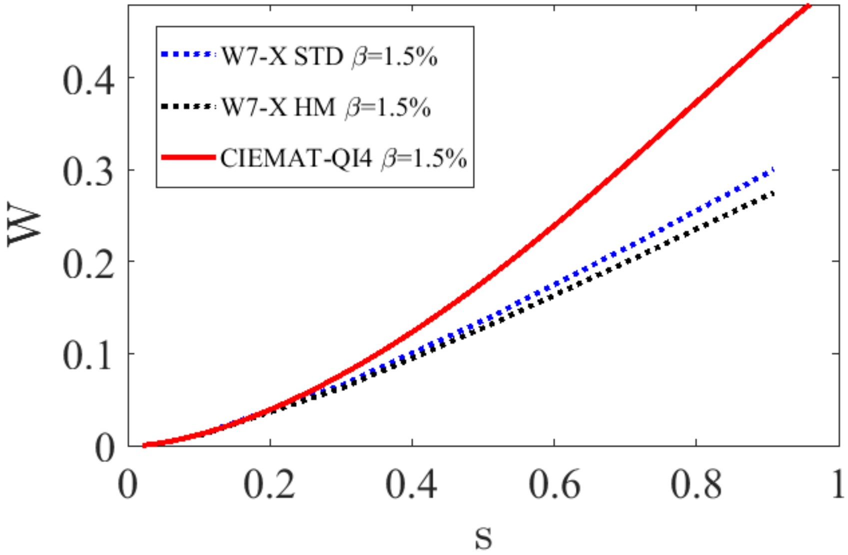

- **The rotational transform profile** (4/5 < ι < 4/4) avoids low order rationals and **would allow an island divertor** at the edge.

- **Positive magnetic well**, larger than that of W7-X HM/STD at β=1.5%, **suporting MHD stability**.

  Mercier stability (D_M >0) increasing with β.

  + Confirmed ballooning stability with COBRA up to β=5%.

$s = \Psi_t/\Psi_{tLCFS} = (r/a)^2$ normalized toroidal flux, used as radial coordinate, with and *a* the minor radius.

Closeness to QI and flat mirror

Magnetic fiel strength over the flux surface

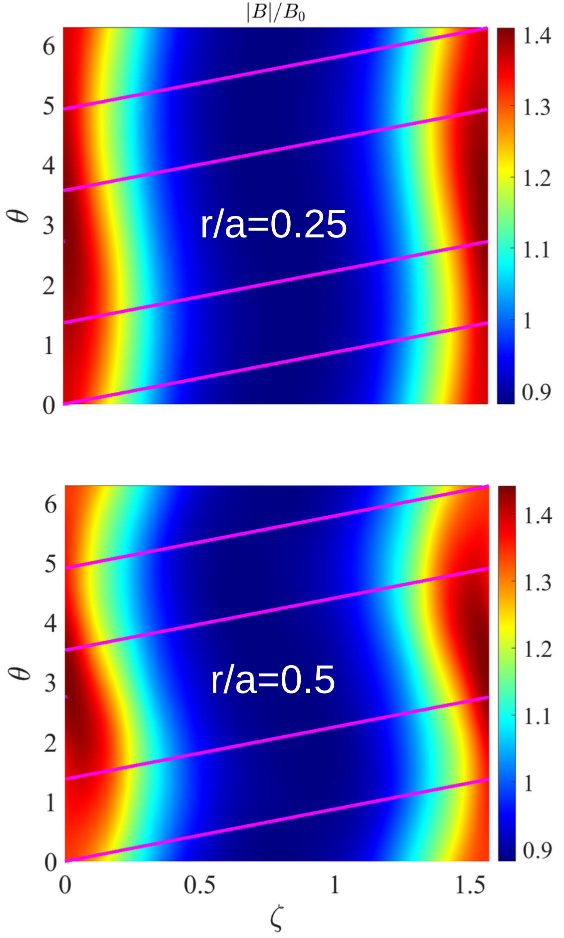

magnetic field strength along the field line

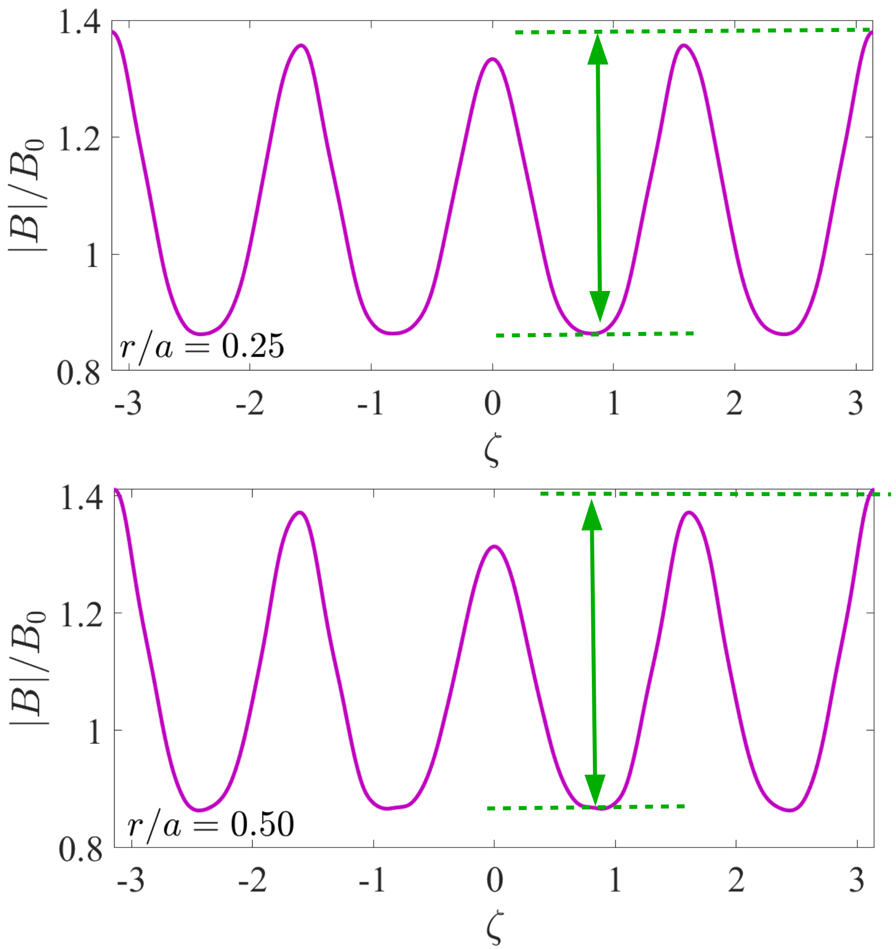

Contours of constant *B* closing poloidally (QI).

Good alignment of *B* maxima.

Small deviations of this alignment (deviation from QI) are tolerable thanks to flat mirror property).

Very good alignment of *B* minima.

Small radial variation of mirror term (**flat mirror property**)

Flat mirror property

- CIEMAT-QI4 belongs to a family of configurations having the flat mirror property, thus benefiting from robust optimization.

  (see Velasco P2.11, this conference).

  - Smaller radial variation of the mirror term than for W7-X HM configuration
  - The radial variation of the mirror decreases with β (see figure).

- Configurations with other periodicities belonging to the same family have already been found: CIEMAT-QI5

  (see Godino-Sedano, P2.24, this conference).

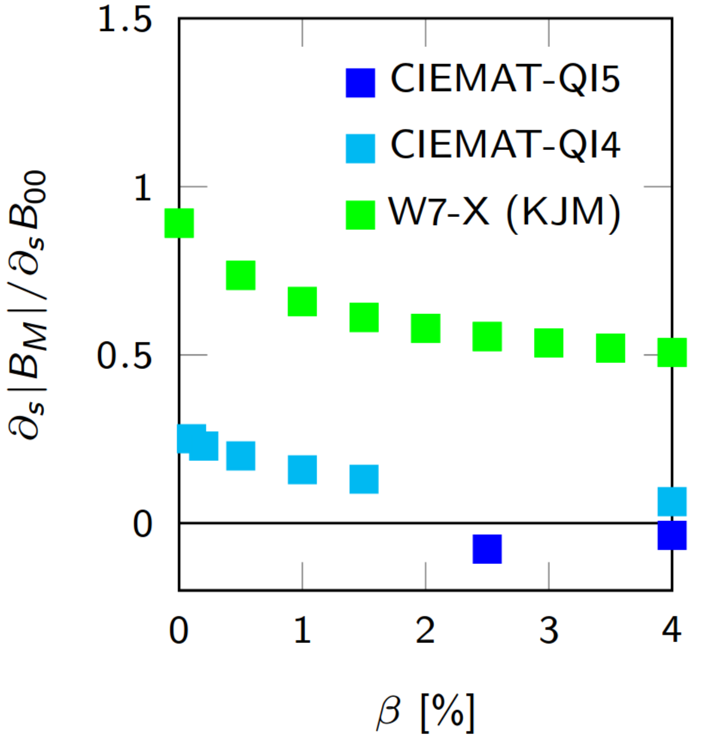

Quantities evaluated at s=0.1

Closeness to QI and maximum-J

As a consequence of $\left|\frac{\partial_\alpha J}{\partial_s J}\right| \ll 1$, we have:

- Alignment of *J* contours with flux surfaces (approach to QI) improving with β.
- *J* contours are closed already for low β.
- *J* is maximum at the axis (s=0) → **Maximum-*J* property**

Reference “exact” QI
with maximum-*J*

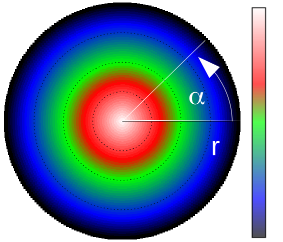

Contours of second adiabatic invariant *J* for E/μ=B_{00} at three different values of β (polar coordinates s,α)

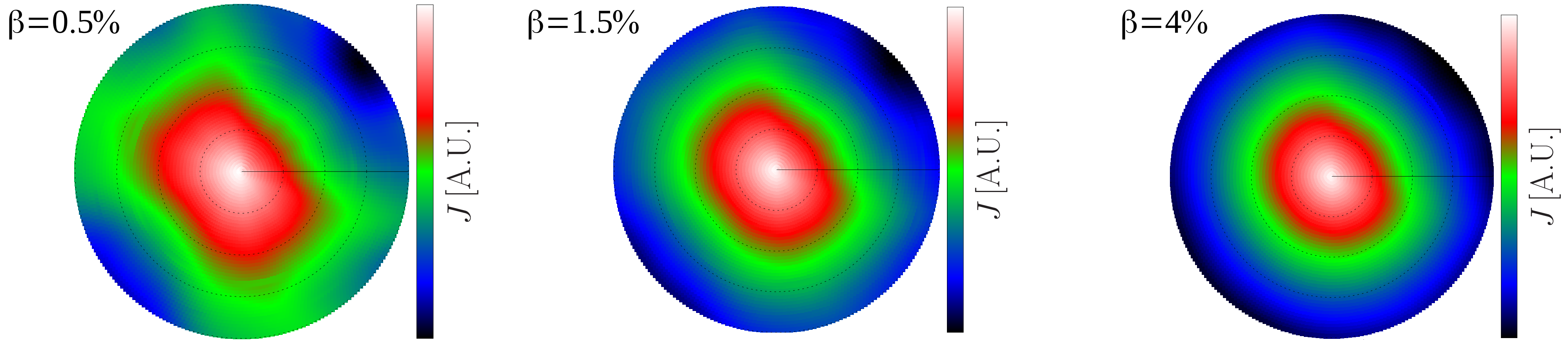
β=0.5%

β=1.5%

β=4%

Neoclassical transport

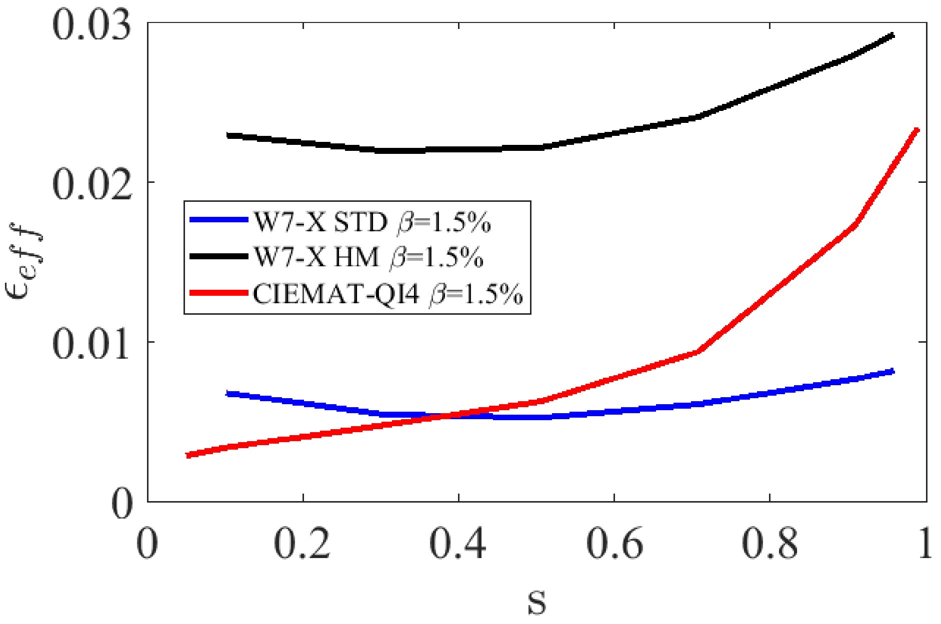

- We use the effective ripple ε_{eff} as a metric of the neoclassical transport for thermal species (push toward omnigeneity).
- The **effective ripple is ε_{eff} < 0.5% for r/a<0.5:**
  - smaller than that of W7-X HM (too large for a reactor)
  - comparable to that of W7-X STD (low enough for a reactor).
- Thanks to the maximum-*J* property, the **neoclassical transport is better than the prediction based on ε_{eff}** for E_r=0 (NC transport equivalent to ε_{eff}=0.0005) [Velasco et al. arXiv:2306.17506v1].

see Velasco P2.11 This conference.

Evaluation of bootstrap current

- The bootstrap current is evaluated with DKES through the coefficient D^*_{31} (E_r=0, β=1.5%*).

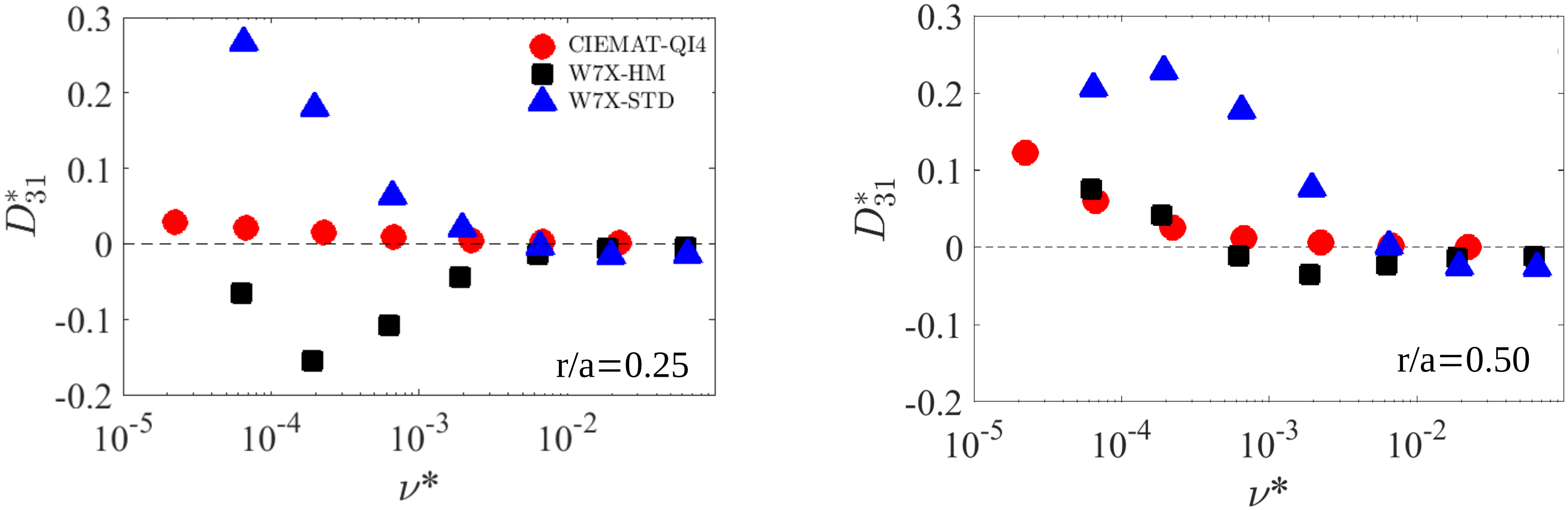

- The bootstrap current in the **CIEMAT-QI4 optimized configuration** is expected to be smaller than that of **W7-X STD** or **HM** configurations.
  - Better control of the rotational transform profile, thus allowing for an island divertor.

* W7-X HM and STD vacuum configurations

FI confinement: ASCOT simulations

- **Losses of fast ions born r/a=0.25.**
  - Very good confinement at β=1.5%, much better than W7X STD or HM at β=1.5%.

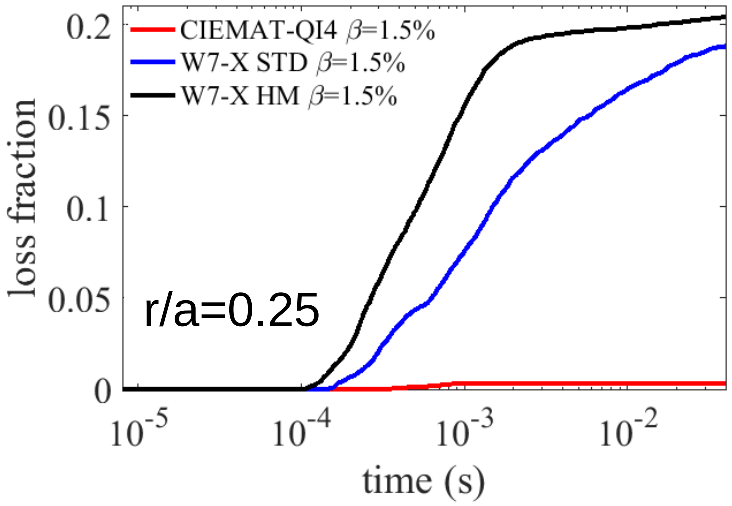

Losses of fast ions born at middle radius (r/a=0.5)

For β=1.5%, losses are significantly smaller than for W7-X (HM or STD).

Tiny loss fraction of fast ions for **β=4% (~1e-3).**a

FI confinement: ASCOT simulations

- **Losses of fast ions born r/a=0.25.**
  - Very good confinement at β=1.5%,

    much better than W7X STD or HM at β=1.5%.

  - Even at β=0.1%, the FI confinement is better than that of W7X STD or HM β=1.5%.

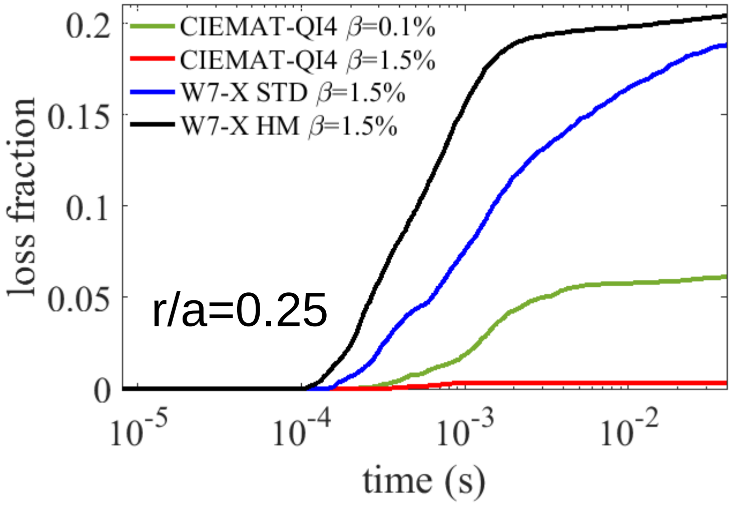

Losses of fast ions born at middle radius (r/a=0.5)

For β=1.5%, losses are significantly smaller than for W7-X (HM or STD).

Tiny loss fraction of fast ions for **β=4% (~1e-3)**.a

FI confinement: ASCOT simulations

- **Losses of fast ions born r/a=0.25.**
  - Very good confinement at β=1.5%,
    much better than W7X STD or HM at β=1.5%.
  - Even at β=0.1%, the FI confinement is better than that of W7X STD or HM β=1.5%.
  - **At reactor scale (β=4%) no fast ions are lost after 0.05 seconds.**

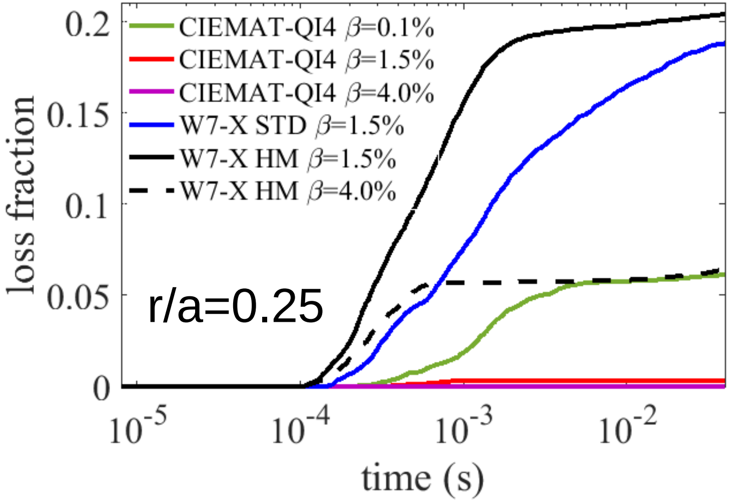

Losses of fast ions born at middle radius (r/a=0.5)

For β=1.5%, losses are significantly smaller than for W7-X (HM or STD).

Tiny loss fraction of fast ions for β=4% (~1e-3).a

FI confinement: ASCOT simulations

- **Losses of fast ions born r/a=0.25.**
  - Very good confinement at β=1.5%, much better than W7X STD or HM at β=1.5%.
  - Even at β=0.1%, the FI confinement is better than that of W7X STD or HM β=1.5%.
  - **At reactor scale (β=4%) no fast ions are lost after 0.05 seconds.**
- **Losses of fast ions born at middle radius (r/a=0.5)**
  - For β=1.5%, losses are significantly smaller than for W7-X (HM or STD).
  - Negligible loss fraction of fast ions for **β=4%** (~10^{-3}).

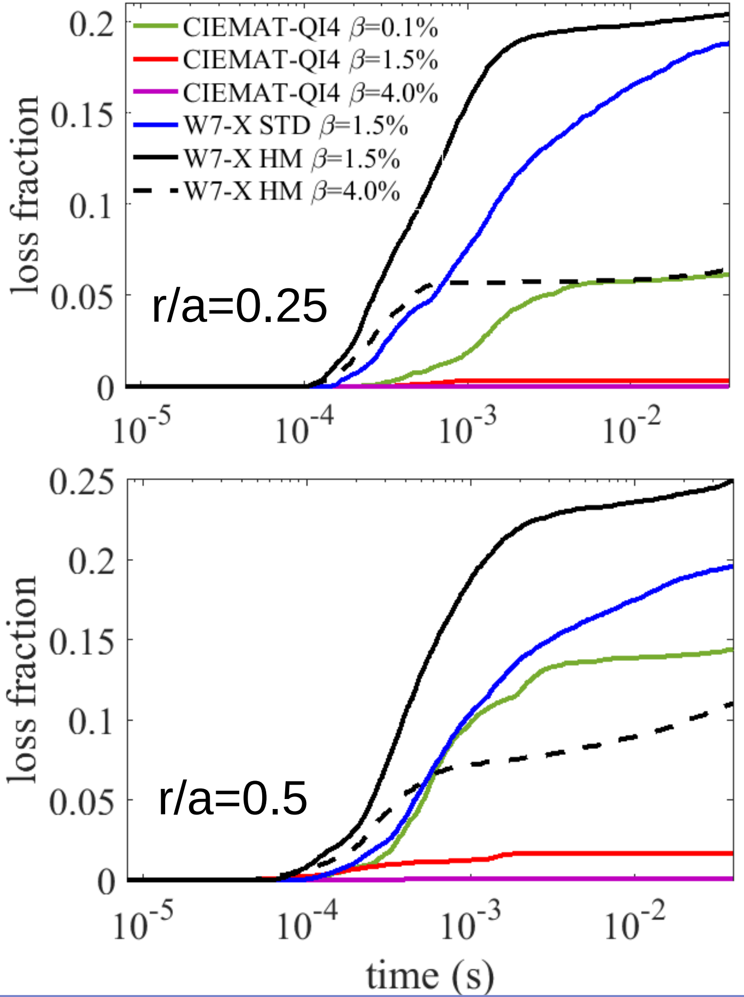

Turbulent transport: stella simulations

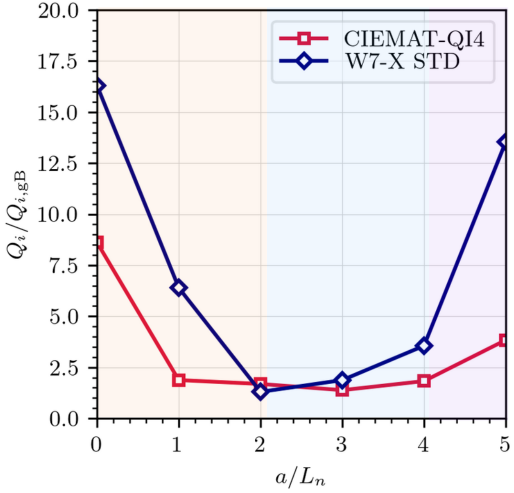

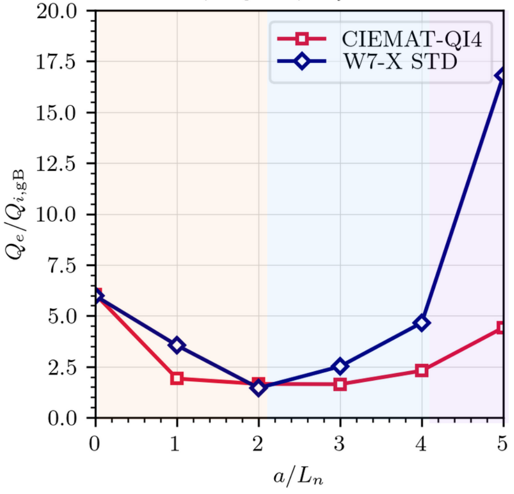

stella [Barnes JCP 2019] flux tube nonlinear simulations with kinetic ions (H^+) and electrons (β=1.5%, r/a=0.7, $a/L_{Ti} = a/L_{Te} = 3$, scan in a/L_n).

- Reduced ion and electron heat fluxes w.r.t. W7-X:
  - Low n_e-gradient: much lower ion heat flux, and comparable or lower electron heat flux than W7-X.
  - Moderate to large n_e-gradient: comparably low (i and e) heat fluxes.
  - Large n_e-gradient: lower (i and e) heat fluxes than W7-X.

- **The density-gradient-driven TEM and other ion-scale turbulence is reduced** (predicted in [Rosenbluth PoF 1968, Helander PoP 2013, Plunk JPP 2017, Proll JPP 2022]) as a consequence of **the maximum-*J* property, obtained at low β thanks to QI + flat mirror property**.

Turbulent transport: stella simulations

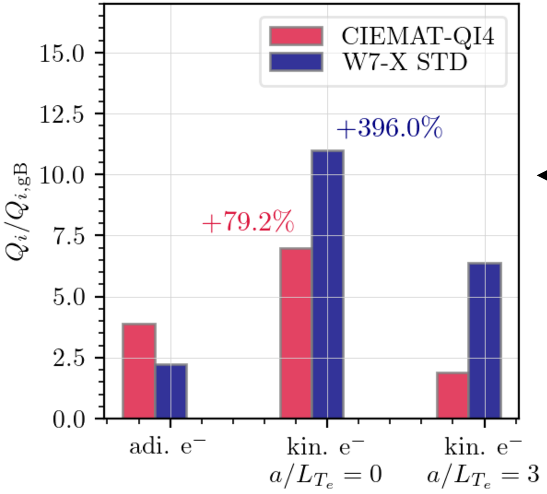

- Kinetic electrons with a flat electron temperature profile strongly increase the ion heat flux.
  - Stronger increase in W7-X than in CIEMAT-QI4.
- Kinetic electrons + electron temperature gradient strongly reduce the ion heat flux w.r.t. the flat-Te case:
  - much stronger reduction in CIEMAT-QI4 than in W7-X.
  - Ion heat flux level **below the adiabatic case in CIEMAT-QI4**.

Stabilization of ion scale modes by kinetic electrons thanks to maximum-*J* property [Rosenbluth PoF 1968, Helander PoP 2013, Plunk JPP 2017, Proll JPP 2022], **obtained at low β thanks to QI + flat mirror property**.

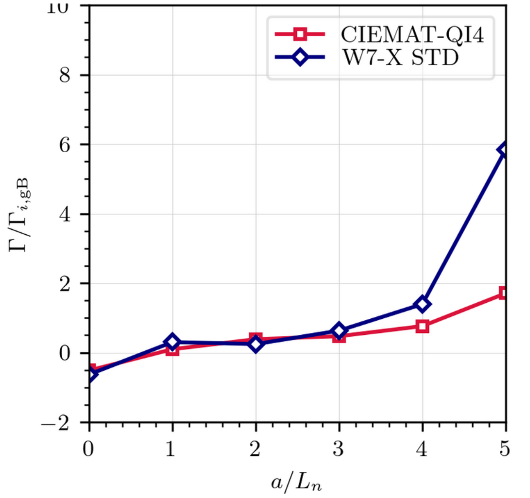

- The particle flux is:
  - Comparably low in CIEMAT-QI4 and W7-X at low density gradient.
  - Smaller in CIEMAT-QI4 for large density gradients (a/L_n>3).

CIEMAT-QI4 could facilitate the formation of a density pedestal without significantly compromising the heat flux.

Preliminary design of filamentary coils

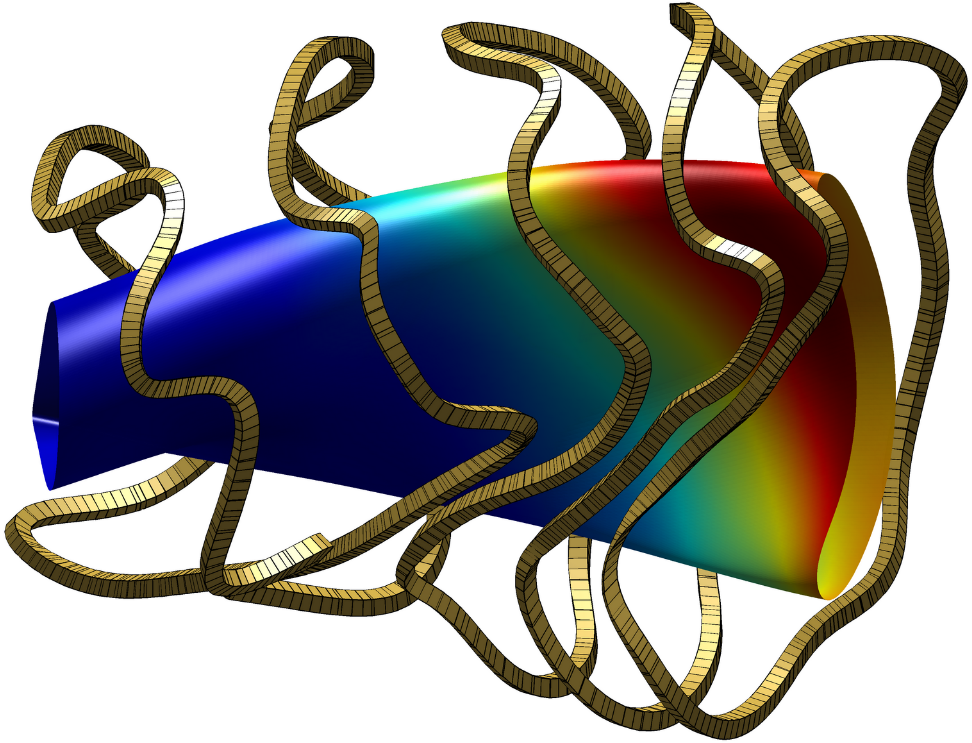

First designs of filamentary coils (5 coils/semiperiod).

Plasma - coils minimum distance ~ plasma minor radius.

- **REGCOIL + Winding Surface (WS) Optimization.**
  - **Magnetic field generated with good fidelity**,
  - Complex coil shapes but, there was room for improvement.

  [Sánchez et al. 2023 Nucl. Fusion 63 066037].

Improved design of filamentary coils

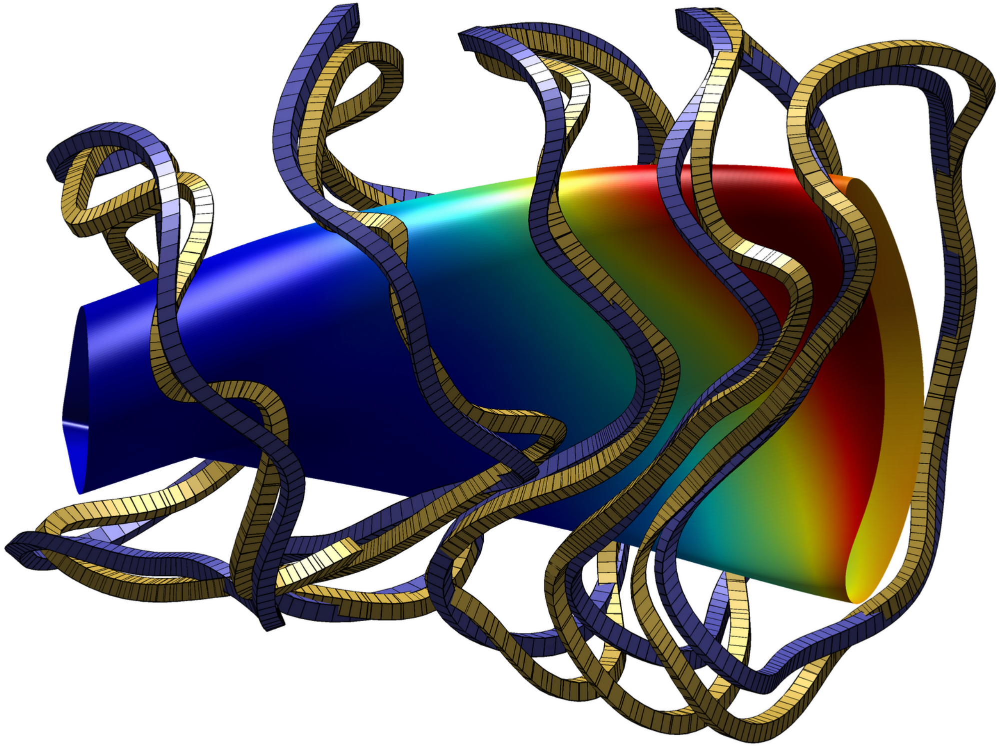

First designs of filamentary coils (5 coils/semiperiod).

Plasma - coils minimum distance ~ plasma minor radius.

- **REGCOIL + Winding Surface (WS) Optimization.**
  - **Magnetic field generated with good fidelity**,
  - Complex coil shapes but, there was room for improvement.

    [Sánchez et al. 2023 Nucl. Fusion 63 066037].
- **Improved coil designs** with FOCUS (New).

Improved design of filamentary coils

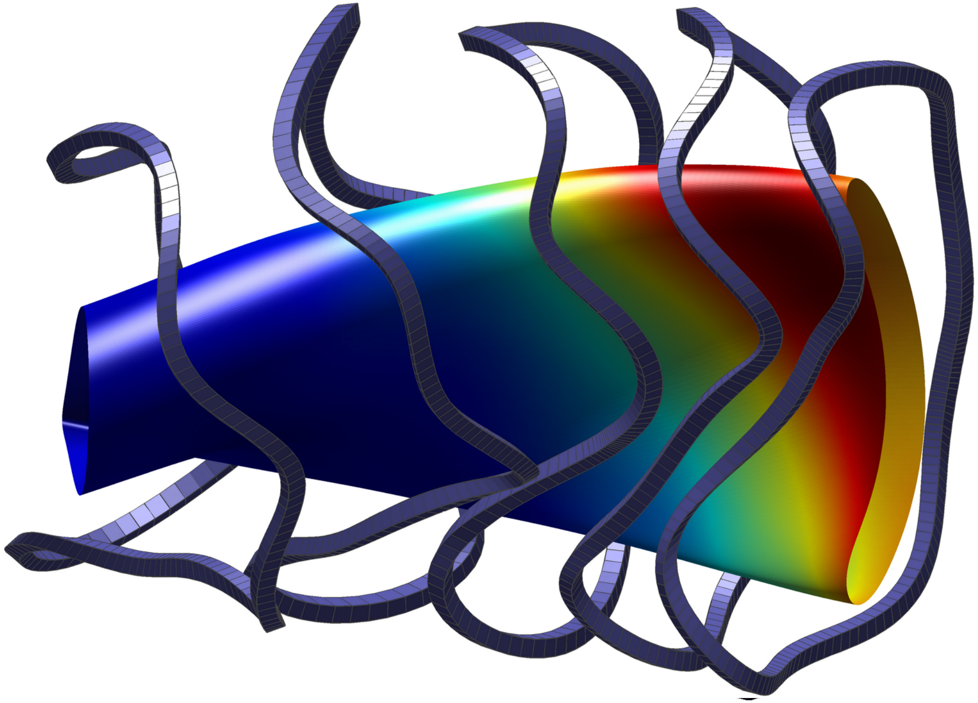

First designs of filamentary coils (5 coils/semiperiod).

Plasma - coils minimum distance ~ plasma minor radius.

- **REGCOIL + Winding Surface (WS) Optimization.**
  - **Magnetic field generated with good fidelity**,
  - Complex coil shapes but, there was room for improvement.

    [Sánchez et al. 2023 Nucl. Fusion 63 066037].
- **Improved coil designs** with FOCUS (New).
  - Reduced maximum curvature.
  - Reduced coil complexity.
  - Improved fidelity, keeping
    - Maximum-*J* property.
    - Reduced bootstrap current.
    - Good fast ion confinement.

Preliminary study for a breeding blanket

- In a reactor design, coils have to be sufficiently separated from the plasma to hold the breeding blanket (BB) and shielding in between, which usually impacts the minimum size (and cost).
- Preliminary models and assesment for CIEMAT-QI4 configuration scaled to reactor size.
  - Model based on winding surface for first set of coils [Sánchez et al. NF 2023].
  - 4 periods, 40 coils, R=16 m, A=9.94.
  - 2750 MW, neutron source: 9.78 10^{20} n/s.
  - Minimum thickness of BB+shielding: 1500 mm.
  - BB thickness: 770 mm.
  - Tritium breeding rate (TBR): 1.39 (1.15 is commonly considered sufficient).

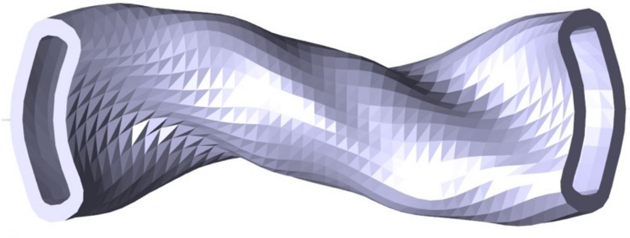

Preliminary study for a breeding blanket

- In a reactor design, coils have to be sufficiently separated from the plasma to hold the breeding blanket (BB) and shielding in between, which usually impacts the minimum size (and cost).
- Preliminary models and assesment for CIEMAT-QI4 configuration scaled to reactor size.
  - Model based on winding surface for first set of coils [Sánchez et al. NF 2023].
  - 4 periods, 40 coils, R=**16** m, A=**9.94**.
  - 2750 MW, neutron source: 9.78 10^{20} n/s.
  - Minimum thickness of BB+shielding: **1500** mm.
  - Minimum BB thickness: **770** mm.
  - Tritium breeding rate (TBR): **1.39** (1.15 is commonly considered sufficient).
- Comparison with HELIAS 5B [Warmer et al. FED 2017]:
  - 5 periods, 50 coils, R=**22** m, A=**12.2**.
  - 3000 MW, neutron source=1.065 10^{21} n/s.
  - Minimum thickness of BB+shielding: **967** mm.
  - Minimum BB thickness: **500** mm.
  - TBR: **1.14 - 1.27** [Palermo et al. NF 2021].

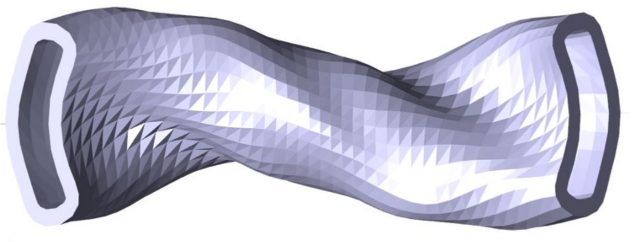

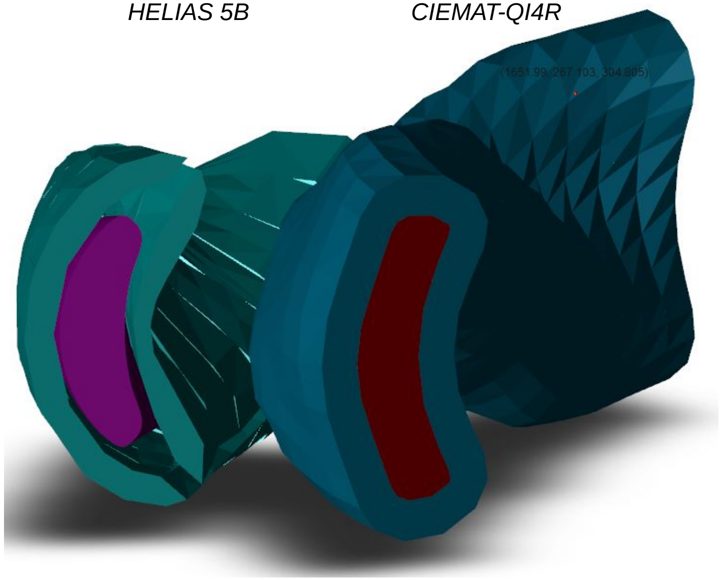

Summary and future work

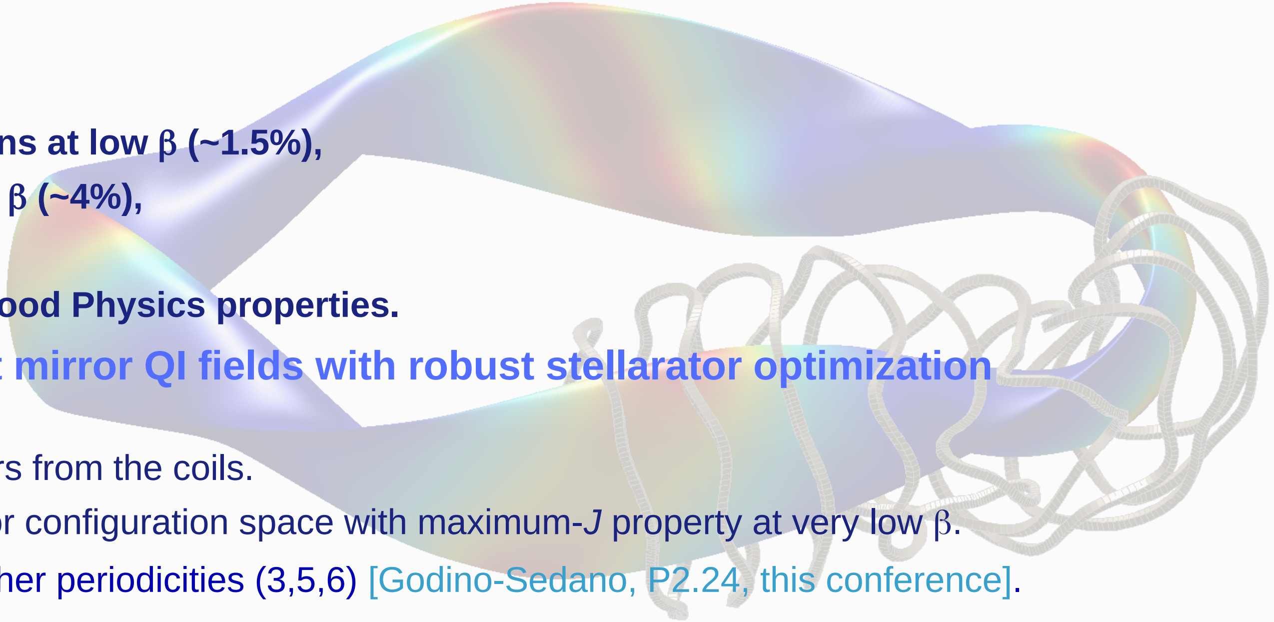

- **CIEMAT-QI4** is the first QI configuration that simultaneously has:
  - rotational transform profile avoiding low-order rationals and, in principle, compatible with an island divertor,
  - ideal MHD stability,
  - low neoclassical transport,
  - reduced bootstrap current,
  - **very good confinement of energetic ions at low β (~1.5%),**
  - **excellent confinement at reactor-scale β (~4%),**
  - **reduced turbulent transport.**
  - **filamentary coil designs keeping the good Physics properties.**
- CIEMAT-QI4 belongs to a family of **flat mirror QI fields with robust stellarator optimization** [Velasco, P2.11, this conference].
  - Resilient to changes with β and field errors from the coils.
  - Previously overlooked region of stellarator configuration space with maximum-*J* property at very low β.
  - Ongoing: exploring configurations with other periodicities (3,5,6) [Godino-Sedano, P2.24, this conference].
- **Step forward in stellarator optimization**: a nearly QI configuration that is compatible with other criteria required for a stellarator reactor.
  - Preliminary calculations of a breeding blanket based on this configuration provide a promising value of TBR.

Thank you!